Macromolecules

Article

pubs.acs.org/Macromolecules

A Novel Benzo[1,2-*b*:4,5-*b*′]dithiophene-Based Conjugated Polymer with a Pendant Diketopyrrolopyrrole Unit for High-Performance Solar Cells

Hua Tan,[†] Xianping Deng,[†] Junting Yu,[†] Baofeng Zhao,[‡] Yafei Wang,[†] Yu Liu,[†] Weiguo Zhu,*[,†] Hongbin Wu,*[,‡] and Yong Cao*[,‡]

[†]Key Lab of Environment-Friendly Chemistry and Application of the Ministry of Education, College of Chemistry, Xiangtan University, Xiangtan 411105, China

[‡]Institute of Polymer Optoelectronic Materials and Devices, State Key Laboratory of Luminescent Materials and Devices, South China University of Technology, Guangzhou 510640, China

Supporting Information

ABSTRACT: A novel conjugated polymer of PBDT-TDPP-S was synthesized, which contains a donor unit of benzo[1,2-*b*:4,5-*b*′]dithiophene in main chain and an acceptor unit of diketopyrrolopyrrole in side chain. This kind of side-chain donor−acceptor (D−A) polymer exhibited better solution processability, lower HOMO level (−5.34 eV), and more balanced carrier mobility relative to its corresponding main-chain D−A conjugated polymers. Using PBDT-TDPP-S as electron donor and [6,6]-phenyl-C_{71}-butyric acid methyl ester ($PC_{71}BM$) as electron acceptor, the resulting polymer solar cells exhibited outstanding photovoltaic properties with a power conversion efficiency of 4.89%, an open-circuit voltage of 0.84 V, a short-circuit current of 10.04 mA cm^{-2}, and a fill factor of 56.0%.

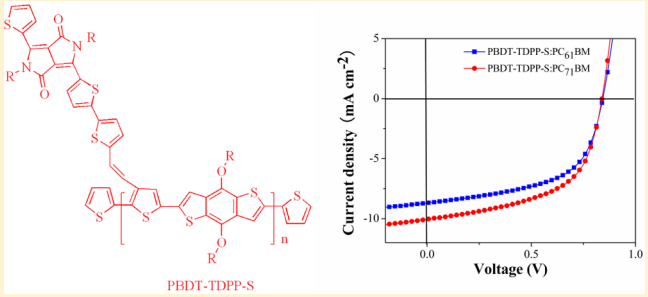

1. INTRODUCTION

Bulk heterojunction (BHJ) polymer solar cells (PSCs) have attracted significant attention because of their potential for achieving large-area, flexible photovoltaic devices through low-cost solution processing techniques.[1] To date, solar power conversion efficiencies (PCE) of 10.6% and 9.2% have been demonstrated in the cells with tandem and single junction structures, respectively, representing an important advance in the development of PSCs.[2] Many recent research efforts have been concentrated on the development of donor−acceptor (D−A) narrow band gap (NBG) polymers with broad absorption spectra.[3] Despite the great success of these D−A polymers in achieving high performance PSCs, further development of novel electron donor polymers is still in urgent need as the donor polymers play a decisive role in determining the device performance.

Nowadays, most of the present polymers are in main-chain D−A frame, which may suffer from lower hole mobility due to the influence of acceptor units in the main chain. Aiming at investigating the effects of the D−A framework on device performance, Huang and co-workers proposed a new molecular design strategy toward side-chain D−A conjugated polymers, in which D moieties were employed to construct the main chain and A units were conjugatedly pended onto the D units in the side chain.[4] Compared to the corresponding main-chain D−A polymers, the side-chain ones mainly possesses three advantages. First, the highest occupied molecular orbit (HOMO) energy levels of the side-chain polymers can preserve in a deeper position. Second, a two-dimensional-like structural feature renders this class of polymers with better solubility. Finally, there exists an internal charge transfer (ICT) behavior from the side-chain D−A structure, which can fine-tune the band gap (E_g) of the resultant polymers as well as promote an isotropic charge transport along the polymeric main chain. As a result of these merits, PSCs based on these previously reported side-chain D−A polymers exhibited a maximal PCE of 4.74%.[4,5]

Nevertheless, most of these side-chain D−A conjugated polymers did not exhibit comparable device performance to their main-chain D−A counterpart polymers. In order to develop high-performance side-chain D−A conjugated polymers, it is necessary to develop new catalog of side-chain D−A polymers for efficient PSCs. Given that benzo[1,2-*b*:4,5-*b*′]dithiophene (BDT) unit has a large planar molecular structure by fusing a benzene with two flanking thiophenyl units and diketopyrrolopyrrole (DPP), i.e., pyrrolo[3,4-*c*]-pyrrole-1,4(2*H*,5*H*)-dione unit has a well conjugated structure with strong $\pi-\pi$ interaction and electron-withdrawing effect, some main-chain D−A copolymers based on DPP or/and BDT

Received: October 29, 2012
Revised: December 14, 2012
Published: December 24, 2012

Scheme 1. Synthetic Route of PBDT-TDPP-S and PBDT-DPP by Stille Cross-Coupling Reaction

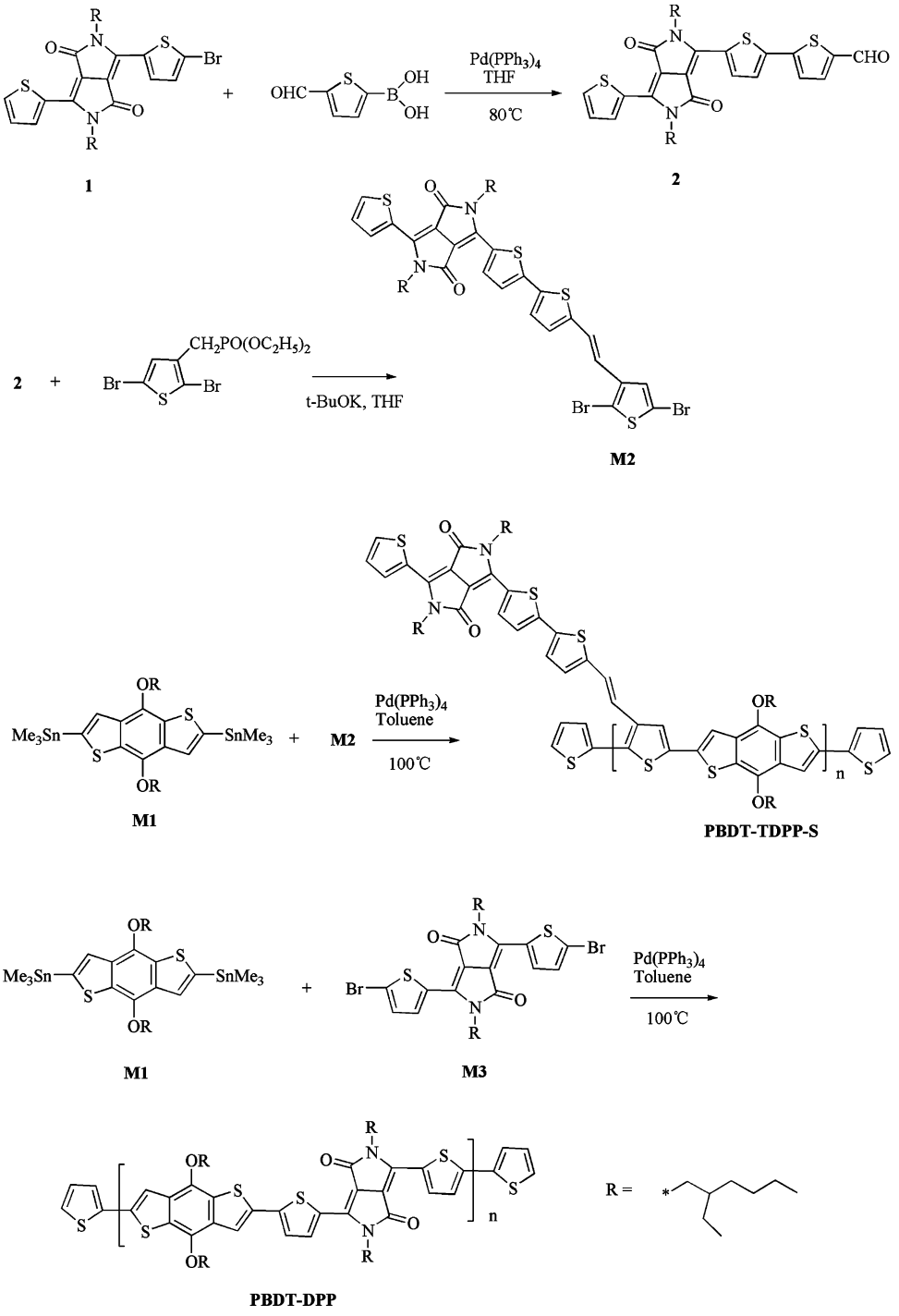

units as prime building block had been designed for optoelectronic applications in both thin-film transistors and solar cells in recent years.[6] It is worthy to note that PSCs based on these copolymers with a tandem structure showed an increasing PCE of 8.62% .[2a] Here we report another novel side-chain D−A conjugated copolymer (PBDT-TDPP-S) for high-performance PSCs, in which the BDT and thiophene units are conjugatedly formed the main chain and the di(thiophen-2-yl)pyrrolo[3,4-*c*]pyrrole-1,4(2*H*,5*H*)-dione (TDPP) units are pended onto the thiophenyl units to build the side chain by a linkage of a 2-vinylthiophenyl unit. Using PBDT-TDPP-S as electron donor and $PC_{71}BM$ as electron acceptor, the resulting PSCs exhibited outstanding photovoltaic properties with a PCE of 4.89%, an open-circuit voltage (V_{OC}) of 0.84 V, a short-circuit current (J_{SC}) of 10.04 mA cm^{-2}, and a fill factor (FF) of 56.0%. To our best knowledge, the efficiency is among the highest reported to date for side-chain D−A conjugated copolymers and is twice higher than that of the main-chain D−A counterpart polymer PBDTDPP-OR in the single BHJ PSCs.[7]

2. RESULTS AND DISCUSSION

2.1. Polymer Synthesis and Thermal Property. The side-chain D−A conjugated copolymer of PBDT-TDPP-S was

dx.doi.org/10.1021/ma302243r | *Macromolecules* 2013, 46, 113−118

synthesized by a common Stille coupling reaction using $Pd(PPh_3)_4$ as catalyst with a high yield of 78.7%, as shown in Scheme 1. For comparison, the corresponding main-chain D−A conjugated copolymer of PBDT-DPP was made at the same time. The resulting PBDT-TDPP-S showed good solubility in common organic solvents, such as chlorobenzene, *o*-dichlorobenzene, and dichloromethane (DCM), but PBDT-DPP was nearly not soluble in them. Gel permeation chromatography (GPC) analysis showed that PBDT-TDPP-S has a number-average molecular weight (M_n) of 1.34×10^4 g mol^{-1} with a polydispersity index of 1.27 (Figure S1). Thermogravimetric analysis (TGA) indicated that PBDT-TDPP-S has high thermal stability with a degradation temperature (T_d) of 364 °C at 5% weight loss. The corresponding molecular weights and thermal properties of PBDT-TDPP-S are summarized in Table 1, and the recorded TGA curve is shown in Figure S2 (see Supporting Information).

Table 1. Molecular Weights and Thermal Properties of Polymers

polymer	$M_n{}^a$ ($\times 10^4$)	$M_w{}^a$ ($\times 10^4$)	PDI^a	$T_d{}^b$ (°C)
PBDT-TDPP-S	1.34	1.70	1.27	364

$^a M_n$, M_w, and PDI were determined by GPC using polystyrene standards with THF as eluent. ^{b}The temperature at 5% weight loss under nitrogen.

2.2. Optical Properties. The UV−vis absorption spectra of PBDT-TDPP-S in DCM solution and solid film are shown in Figure 1a. Their corresponding UV absorption data are listed in Table 2. In DCM solution, PBDT-TDPP-S shows two obvious absorption peaks. The first one at ∼420 nm corresponds to the $\pi-\pi^*$ transition of the polymeric backbone in short wavelength region. The second one at ∼590 nm in long wavelength region is attributed to the ICT interaction between the donor unit in the main chain and the acceptor unit at the side chain. Compared with the absorption spectrum in DCM solution, the one in solid film displayed a red-shift absorption peak at 602 nm and an additional shoulder at 655 nm besides the high-energy peak. The extended absorption edge in long wavelength region can be attributed to the more aggregated configuration formed in solid state. Compared to the main-chain copolymer of PBDTDPP-OR reported by the Jo group, this side-chain copolymer of PBDT-TDPP-S exhibited a 100 nm blue-shifted maximum absorption peak. The observed blue-shifted absorption phenomenon should be related to the less planar conformation and weaker D−A interaction for the side-chain D−A copolymer than the main-chain D−A copolymer. As a result, the optical band gap (E_g^{opt}) of PBDT-TDPP-S was shifted to 1.73 eV as calculated from the onset of absorption spectra in the solid film.

2.3. Electrochemical Properties. The electrochemical cyclic voltammetry (CV) curve of the PBDT-TDPP-S film coated on a platinum electrode is shown in Figure S3 (see Supporting Information), and the electrochemical data are also summarized in Table 2. An onset oxidation potential of 0.94 V and an onset reduction potential of −0.88 V (vs SCE) are observed. Based on an empirical formula, the corresponding HOMO and the lowest unoccupied molecular orbital (LUMO) energy levels (E_{HOMO} and E_{LUMO}) of PBDT-TDPP-S were calculated to be −5.34 and −3.52 eV, respectively. This resulting E_{HOMO} level is lower than those of the reported main-chain D−A copolymers of PDPP-BDT (−5.16 eV) and

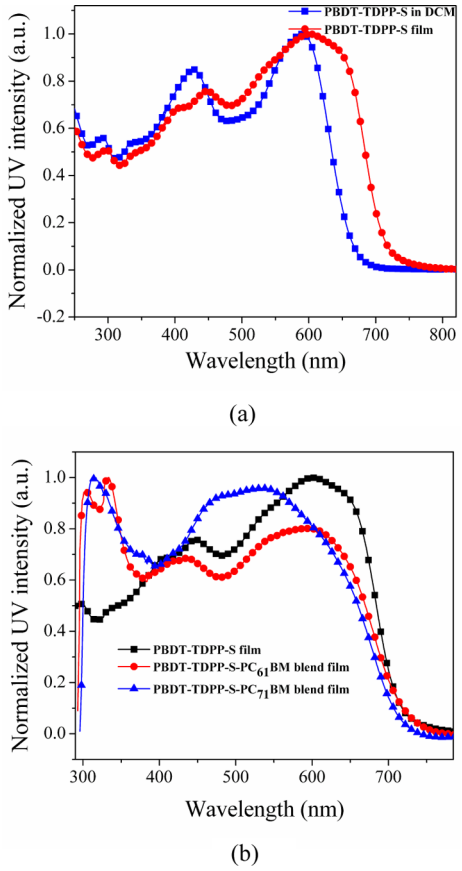

Figure 1. Normalized UV−vis absorption spectra of PBDT-TDPP-S in DCM and in the neat film at RT (a). UV−vis absorption spectra of the PBDT-TDPP-S/$PC_{61}BM$ and the PBDT-TDPP-S/$PC_{71}BM$ blend films with a weight ratio of 1:1.3 (b).

PBDTPP-OR (−5.29 eV).[8] The relatively low E_{HOMO} for PBDT-TDPP-S is beneficial to achieve high V_{OC} in PSCs, given the strong correlation between the V_{OC} and the difference between the E_{HOMO} of donor and the E_{LUMO} of acceptor in PSCs.[8]

2.4. Photovoltaic Properties. The photovoltaic properties of the PBDT-TDPP-S were studied in PSCs using $PC_{61}BM$ or $PC_{71}BM$ as an acceptor. The device configuration was ITO/PEDOT:PSS (30 nm)/polymer:acceptor (80 nm)/LiF(0.7 nm)/Al(100 nm). The effective device area was 7×10^{-2} cm^2, as defined by a shadow mask. In order to understand the influence of ratios between the donor polymer and acceptor, thicknesses of the photoactive layer, and the annealing temperatures on the photovoltaic properties, the current density−voltage ($J-V$) characteristics of the PBDT-TDPP-S:$PC_{71}BM$-based devices at different ratios, thicknesses, and annealing temperatures are shown in Figures S4, S5, and S6, respectively. The resulting photovoltaic data are summarized in Tables S1, S2, and S3, respectively. The optimized ratio of 1:1.3, thickness of 80 nm, and annealing temperature of 120 °C were obtained. In these optimized conditions, two typical devices using $PC_{71}BM$ and $PC_{61}BM$ as acceptor exhibited the following typical $J-V$ characteristics in Figure 2 under 1000 W m^{-2} air mass 1.5 global (AM 1.5G) illumination. Device parameters, such as J_{SC}, V_{OC}, FF, and PCE are deduced from the $J-V$ characteristics and summarized in Table 3.

It is clear that the PBDT-TDPP-S:$PC_{71}BM$-based devices exhibited better photovoltaic properties as compared to the

dx.doi.org/10.1021/ma302243r | *Macromolecules* 2013, 46, 113−118

Table 2. Optical and Electrochemical Properties of PBDT-TDPP-S

polymer	λ_{max}/nm (solution)	λ_{max}/nm (film)	$E_{g\ (opt)}{}^{a}$/V	E_{ox}/V	E_{red}/V	$E_{HOMO}{}^{b}$/eV	$E_{LUMO}{}^{c}$/eV	$E_{g(elec)}{}^{d}$/eV
PBDT-TDPP-S	427, 588	445, 598	1.73	0.94	−0.88	−5.34	−3.52	1.82

[a]Optical energy gap determined from the onset position of the absorption band. [b]HOMO position (vs SCE) determined from onset of oxidation. [c]LUMO position (vs SCE) determined from onset of reduction. [d]Electrochemical energy gap.

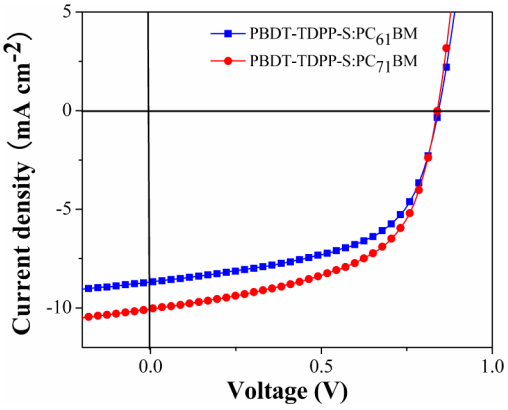

Figure 2. Current density−voltage (J−V) characteristics of the devices at a 1:1.3 weight ratio between PBDT-TDPP-S and $PC_{61}BM$/$PC_{71}BM$ under simulated AM 1.5G illumination (1000 W m^{-2}).

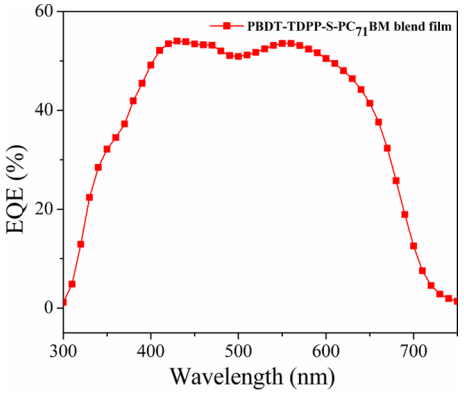

Figure 3. External quantum efficiency curve of the PBDT-TDPP-S/$PC_{71}BM$-based PSCs.

PBDT-TDPP-S:$PC_{61}BM$-based devices, which can be attributed to the stronger absorption of $PC_{71}BM$ than $PC_{61}BM$ in the visible region from 440 to 530 nm, as shown in Figure 1b. A maximal PCE of 4.89% with an V_{OC} of 0.84 V, a J_{SC} of 10.04 mA cm^{-2}, and a FF of 56.0% was achieved for the PBDT-TDPP-S:$PC_{71}BM$-based devices. To our best knowledge, the recorded maximum PCE and FF levels here are higher than those for the previous side-chain D−A conjugated copolymers-based PSCs. Furthermore, these PSCs based on the side-chain D−A polymer of PBDT-TDPP-S presented significantly improved device performance over those PSCs using a main-chain D−A polymer of PDPP-BDT or PBDTPP-OR as donor.[7] Figure 3 shows the external quantum efficiency (EQE) curve of the device with the PBDT-TDPP-S: $PC_{71}BM$ blend. The EQE values are about 45% with a broad response from 300 to 750 nm, which are consistent with the optical absorption profile in Figure 1b. According to the EQE curve and the solar irradiation spectrum, the integral current density value of the device is 9.70 mA cm^{-2}. The difference between the measured J_{SC} and the integral current density values is within 3%. It indicates that our photovoltaic measurement is accurate and reliable. The moderate EQE reported here implies some potential for further enhancement in J_{SC} as well.

To assess the charge transport properties for the PBDT-TDPP-S:$PC_{71}BM$ blend used as photoactive layer, we measured the J−V characteristics of single charge carrier devices at room temperature and applied space-charge-limited-current (SCLC) model to extract the charge carrier mobility.[1i] Figure 4 shows the J−V (a) and $J^{1/2}$−V (b) characteristics of the PBDT-TDPP-S devices with a hole-only device configuration of ITO/PEDOT:PSS (40 nm)/active layer (varied thickness)/ MoO_3/

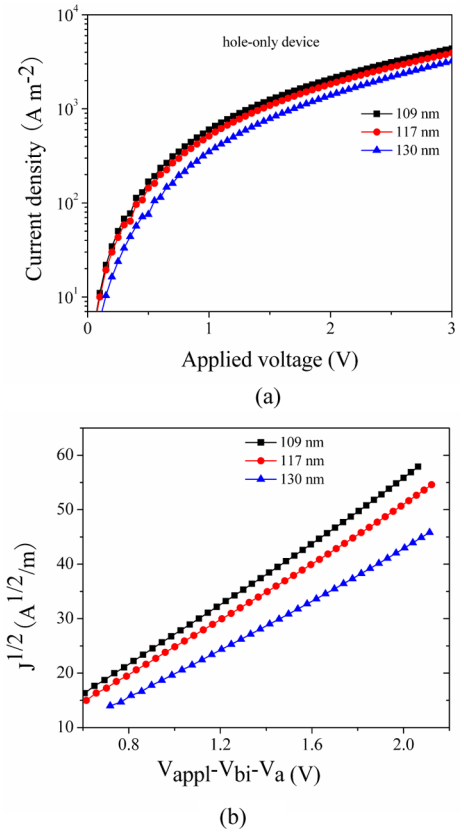

Figure 4. (a) J−V and (b) $J^{1/2}$−V characteristics of the PBDT-TDPP-S hole-only devices with different thicknesses measured at ambient temperature.

Table 3. Photovoltaic Properties of the PBDT-TDPP-S-Based PSCs

donor	acceptor	thickness/nm	J_{sc}/mA cm^{-2}	V_{oc}/V	FF/%	PCE_{max}/%
PBDT-TDPP-S	$PC_{61}BM$	80	8.67	0.84	57.0	4.31
PBDT-TDPP-S	$PC_{71}BM$	80	10.04	0.84	56.0	4.89

dx.doi.org/10.1021/ma302243r | Macromolecules 2013, 46, 113−118

Al(100 nm). Although PBDT-TDPP-S contains bulky and rigid side chains, its blend film with $PC_{71}BM$ exhibited a high hole mobility of 3.8×10^{-4} cm^2 V^{-1} s^{-1}. Moreover, the observed hole mobility is higher than those of the recent reported main-chain D−A polymers,[9] verifying that side-chain D−A polymers can have strong intermolecular orbital overlap and good molecular packing like main-chain D−A polymers. Besides the high hole mobility, the blend also presented high electron mobility in range of 4.4×10^{-4} cm^2 V^{-1} s^{-1} (see Figure S7). The measured hole and electron mobility are listed in Table 4.

Table 4. Charge Transport Properties for the PBDT-TDPP-S:$PC_{71}BM$ Blend Estimated by the SCLC Model

thickness (nm)	109	117	130
hole mobility (cm^2 V^{-1} s^{-1})	3.46×10^{-4}	3.61×10^{-4}	3.82×10^{-4}
electron mobility (cm^2 V^{-1} s^{-1})	3.30×10^{-4}	3.16×10^{-4}	4.46×10^{-4}

Such high and balanced hole−electron mobility for the PBDT-TDPP-S is responsible for the high FF level in the devices. To our best knowledge, the FF is the highest reported to date for side-chain D−A conjugated copolymers

The surface morphology of the active layers was studied using atomic force microscopy (AFM) under tapping mode in order to further understand why the device exhibited better photovoltaic properties at the annealing temperature of 120 °C. Figure S8 shows typical AFM topography of the PBDT-TDPP-S:$PC_{71}BM$ blend film in unannealed and annealed conditions (see Supporting Information). The surface roughness is observed to be 0.773 nm in unannealed condition and 0.602 nm in annealed condition. It indicates that the surface roughness of the blend film can be tuned much smoother by the prethermal annealing. The smooth morphology of the active layer is available for improving the device performance.[10] Therefore, the devices exhibited improved photovoltaic properties by prethermal annealing at an appropriate temperature.

3. CONCLUSION

In summary, a novel conjugated polymer of PBDT-TDPP-S was successfully obtained, which contains a donor unit of benzo[1,2-b:4,5-b′]dithiophene in main chain and an acceptor unit of diketopyrrolopyrrole in side chain. The resultant side-chain D−A polymer exhibited high carrier mobility and outstanding photovoltaic properties in polymer solar cells with a PCE as high as 4.89%. The PCE level is the highest reported to date in the side-chain D−A conjugated copolymers-based single BHJ PSCs, which is twice higher than that of the corresponding main-chain D−A polymer-based ones. Our work presented a new promising side-chain polymeric photovoltaic material for high-performance PSCs.

4. EXPERIMENTAL SECTION

Materials. 2,6-Bis(trimethyltin)-4,8-bis(2-ethylhexyloxy)benzo-[1,2-*b*:4,5-*b*′]dithiophene (**M1**) and 3-(5-bromothiophen-2-yl)-2,5-bis(2-ethylhexyl)-6-(thiophen-2-yl)pyrrolo[3,4-*c*]pyrrole-1,4(2*H*,5*H*)-dione (**1**) were synthesized by the reported procedures.[11,12] Tetrahydrofuran (THF) was distilled over sodium benzophenone under an inert nitrogen atmosphere. Toluene was dried and distilled over sodium under an inert argon atmosphere.

Synthesis of 2. A mixture of **1** (0.60 g, 1.00 mmol), 5-formyl-2-thiopheneboronic acid (0.16 g, 1.0 mmol), and tetrakis-(triphenylphosphine)palladium(0) (0.012 g, 0.01 mmol) was dissolved in 15 mL of THF and mixed with sodium bicarbonate (0.15 g, 1.42 mmol) in 3 mL of water. After stirring for 12 h at 80 °C under argon, the mixture was poured into water and extracted with chloroform. The organic layers were separated, dried over magnesium sulfate, and filtered. The filtrate was distilled to remove the solvent, and the residue was purified by column chromatography using DCM:PE (1:1 to 1:0) as eluent to produce **2** as a purple solid (0.31 g, 49%). ^{1}H NMR (400 MHz, $CDCl_3$, δ): 9.94 (s, 1H), 8.97 (d, J = 4.0 Hz, 1H), 8.90 (d, J = 6.0 Hz, 1H), 7.74 (d, J = 4.4 Hz, 1H), 7.68 (d, J = 4.0 Hz, 1H), 7.50 (d, J = 4.0 Hz, 1H), 7.40 (d, J = 6.4 Hz, 1H), 7.31 (d, J = 3.6 Hz, 1H), 4.03 (t, J = 7.2 Hz, 4H), 1.84−1.98 (m, 2H), 1.50−1.15 (m, 16H), 0.88 (t, J = 6.0 Hz, 12H). MS (MALDI-TOF): Calcd for $C_{35}H_{42}N_2O_3S_3$ $[M]^+$, 634.2; found, 635.2.

Synthesis of M2. A solution of **2** (0.63 g, 1 mmol) and (2,5-dibromothiophen-3-ylmethyl)phosphonic acid diethyl ester (0.39 g, 1 mmol) and THF (20 mL) was stirred and degassed for 30 min at RT under a nitrogen atmosphere. Then another solution of potassium *tert*-butoxide (0.13 g, 1.15 mmol) and THF (20 mL) was dropwise added into it. The resulting mixture was stirred for 5 h at RT and sequentially for 12 h at 60 °C under a nitrogen atmosphere. After being cooled to RT, the mixture was extracted with dichloromethane and washed with dilute HCl aqueous solution. The organic phase was dried over anhydrous $MgSO_4$ and distilled to remove the solvent by rotary evaporation. The residue was purified by silica gel column chromatography using petroleum ether/dichloromethane (3:1) as eluent to give **M2** as a purple solid (0.37g, 42%). ^{1}H NMR (400 MHz, $CDCl_3$, δ): 8.94 (d, J = 4.0 Hz, 1H), 8.89 (d, J = 4.8 Hz, 1H), 7.62 (d, J = 4.4 Hz, 1H), 7.32 (d, J = 4.0 Hz, 1H), 7.27 (d, J = 6.4 Hz, 1H), 7.21 (d, J = 3.6 Hz, 1H), 7.15 (d, J = 4.0 Hz, 1H), 6.93−7.06 (br, 2H), 6.80 (d, J = 6.4 Hz, 1H), 4.03 (t, J = 7.2 Hz, 4H), 1.81−1.98 (m, 2H), 1.49−1.17 (m, 16H), 0.88 (t, J = 8.4 Hz, 12H). MS (MALDI-TOF): Calcd for $C_{40}H_{44}Br_2N_2O_2S_4$ $[M]^+$, 872.1; found, 872.0.

Synthesis of the PBDT-TDPP-S. A mixture of monomers **M1** (77.2 mg, 0.1 mmol), **M2** (87.2 mg, 0.1 mmol), $Pd(PPh_3)_4$ (5 mg), and toluene (3 mL) was degassed with nitrogen flow and stirred at 90 °C for 48 h under a nitrogen atmosphere. After being cooled to RT, tributyl(thiophen-2-yl)stannane (37 mg, 0.10 mmol) was added and the mixture was refluxed for 12 h. Then 2-bromothiophene (32 mg, 0.20 mmol) was injected, and the mixture was refluxed for another 12 h. The mixture was cooled to RT and poured into 200 mL of MeOH to form precipitate. The precipitate was collected and dissolved in DCM. The filtrate was poured into 200 mL of MeOH again to provide precipitate. Then the precipitate was washed with acetone in a Soxhlet apparatus for 48 h to give the PBDT-TDPP-S as black solid (91.1 mg, 78.7%). ^{1}H NMR ($CDCl_3$, 400 MHz, δ): 8.97−8.73 (br, 2H), 7.68−6.84 (br, 12H), 4.30−4.06 (br, 4H), 4.05−3.81 (br, 4H), 1.99−1.10 (br, 36H), 1.10−0.59 (br, 24H). IR: V_{max} (cm^{-1}), 3069 (=C−H), 2956, 2923, 2856 (−C−H), 1663 (−C=O), 1556 (−C=C), 1512, 1453, 1429,1400, 1359, 1226, 1167, 1099, 1067, 1037, 940, 855, 810, 785, 734, 702.

Synthesis of the PBDT-DPP. A mixture of **M1** (77.2 mg, 0.1 mmol), **M3** (68.2 mg, 0.1 mmol), $Pd(PPh_3)_4$ (5 mg), and toluene (3 mL) was degassed with nitrogen flow and stirred at 90 °C for 48 h under a nitrogen atmosphere. After being cooled to RT, tributyl-(thiophen-2-yl)stannane (37 mg, 0.10 mmol) was added and the mixture was refluxed for 12 h. Then 2-bromothiophene (32 mg, 0.20 mmol) was injected, and the mixture was refluxed for another 12 h. The mixture was cooled to RT and poured into 200 mL of MeOH to form precipitate as black solid. Any purification and measurement were not made due to its bad solubility in common organic solvents.

■ ASSOCIATED CONTENT

Ⓢ Supporting Information

Experimental details. This material is available free of charge via the Internet at http://pubs.acs.org.

■ AUTHOR INFORMATION

Corresponding Author

*E-mail: zhuwg18@126.com (W.Z.); hbwu@scut.edu.cn (H.W.); yongcao@ scut.edu.cn (Y.C.).

Notes

The authors declare no competing financial interest.

■ ACKNOWLEDGMENTS

Thanks to the financial support from the Major Program for cultivation of the National Natural Science Foundation of China (91233112), the National Natural Science Foundation of China (21172187, 51273168, 21202139), the Innovation Group and Xiangtan Joint Project in Hunan Natural Science Foundation (12JJ7002 and 12JJ8001), the Hunan Postgraduate Science Foundation for Innovation (CX2011B263), and the Study and Innovation Experimental Program for Undergraduate Students in Hunan (2011and 2012). Special thanks to Prof. Liming Ding and his student Shan Chen in National Center for Nanoscience and Technology. The photovoltaic performance of PSCs devices was characterized under their help.

■ REFERENCES

(1) (a) Zhou, H. X.; Yang, L. Q.; Stuart, A. C.; Price, S. C.; Liu, S. B.; You, W. *Angew. Chem., Int. Ed.* **2011**, *50*, 2995−2998. (b) Facchetti, A. *Chem. Mater.* **2011**, *23*, 733−758. (c) Chochos, C. L.; Choulis, S. A. *Prog. Polym. Sci.* **2011**, *36*, 1326−1414. (d) Cheng, Y.-J.; Chen, C.-H.; Lin, Y.-S.; Chang, C.-Y.; Hsu, C.-S. *Chem. Mater.* **2011**, *23*, 5068−5075. (e) Son, H. J.; Wang, W.; Xu, T.; Y. Liang, Y.; Wu, Y.; Li, G.; Yu, L. P. *J. Am. Chem. Soc.* **2011**, *133*, 1885−1894. (f) Chu, T.-Y.; Lu, J. P.; Beaupré, S.; Zhang, Y. G.; Pouliot, J.-R.; Zhou, J. Y.; Najari, A.; Leclerc, M.; Tao, Y. *Adv. Funct. Mater.* **2012**, *22*, 2345−2351. (g) Chang, C.-Y.; heng, Y.-J.; Hung, C.-H.; Wu, J.-S.; Kao, W.-S.; Lee, C.-H.; Hsu, C.-S. *Adv. Mater.* **2012**, *24*, 549−553. (h) He, Z. C.; Zhong, C.; Xu, X. F.; Zhang, L. J.; Huang, L.; Chen, J. W.; Wu, H. B.; Cao, Y. *Adv. Mater.* **2011**, *23*, 3086−3089. (i) He, Z. C.; Zhong, C. M.; Huang, X.; Wong, W.-Y.; Wu, H. B.; Chen, L. W.; Su, S. J. *Adv. Mater.* **2011**, *23*, 4636−4643.

(2) (a) Dou, L. T.; You, J. B.; Yang, J. C.; Chen, C.-C.; He, Y. J.; Murase, S.; Moriarty, T.; Emery, K.; Li, G.; Yang, Y. *Nat. Photonics* **2012**, *6*, 180−185. (b) He, Z. C.; Zhong, C. M.; Su, S. J.; Xu, M.; Wu, H. B.; Cao, Y. *Nat. Photonics* **2012**, *6*, 593−597.

(3) (a) Min, J.; Zhang, Z.-G.; Zhang, S. Y.; Zhang, M. J.; Zhang, J.; Li, Y. F. *Macromolecules* **2011**, *44*, 7632−7638. (b) Duan, R. M.; Ye, L.; Guo, X.; Huang, Y.; Wang, P.; Zhang, S. Q.; Zhang, J. P.; Huo, L. J.; Hou, J. H. *Macromolecules* **2012**, *45*, 3032−3038. (c) Zhang, J.; Cai, W. Z.; Huang, F.; Wang, E. G.; Zhong, C. M.; Liu, S. J.; Wang, M.; Duan, C. H.; Yang, T. B.; Cao, Y. *Macromolecules* **2011**, *44*, 894−901. (d) Zou, J. Y.; Yip, H.-L.; Zhang, Y.; Gao, Y.; Chien, S.-C.; O'Malley, K.; Chueh, C.-C.; Chen, H. Z.; Jen, A. K. *Adv. Funct. Mater.* **2012**, *22*, 2804−2811. (e) Li, X. H.; Choy, W. C.; Huo, L. J.; Xie, F. X.; Sha, W. E.; Ding, B. F.; Guo, X.; Li, Y. F.; Hou, J. H.; You, J. B.; Yang, Y. *Adv. Mater.* **2012**, *24*, 3046−3052. (f) Liu, J.; Shao, S. Y.; Fang, G.; Meng, B.; Xie, Z. Y.; Wang, L. X. *Adv. Mater.* **2012**, *24*, 2774−2779. (g) Lin, Y. Z.; Fan, H. J.; Li, Y. F.; Zhan, X. W. *Adv. Mater.* **2012**, *24*, 3087−3106.

(4) Huang, F.; Chen, K. S.; Yip, H. L.; Hau, S. K.; Acton, O.; Zhang, Y.; Luo, J.; Jen, A. K. Y. *J. Am. Chem. Soc.* **2009**, *131*, 13886−13887.

(5) (a) Duan, C. H.; Hu, X. W.; Chen, K. S.; Yip, H. L.; Li, W.; Huang, F.; Jen, A. K. Y.; Cao, Y. *Sol. Energy Mater. Sol. Cells* **2012**, *97*, 50−58. (b) Duan, C. H.; Cai, W. Z.; Huang, F.; Zhang, J.; Wang, M.; Yang, T. B.; Zhong, C. M.; Gong, X.; Cao, Y. *Macromolecules* **2010**, *43*, 5262−5268. (c) Duan, C. H.; Chen, K. S.; Huang, F.; Yip, H. L.; Liu, S. J.; Zhang, J.; Jen, A. K.; Cao, Y. *Chem. Mater.* **2010**, *22*, 6444−6452. (d) Zhang, Z. G.; Liu, Y. L.; Yang, Y.; Hou, K. Y.; Peng, B.; Zhao, G. J.; Zhang, M. J.; Guo, X.; Kang, E. T.; Li, Y. F. *Macromolecules* **2010**, *43*, 9376−9383. (e) Sahu, D.; Padhy, H.; Patra, D.; Huang, J. H.; Chu, C. W.; Lin, H. C. *J. Polym. Sci., Part A: Polym. Chem.* **2010**, *48*, 5812−5823. (f) Zhang, Z. G.; Fan, H. J.; Min, J.; Zhang, J.; M. Zhang, J.; Guo, X.; Zhan, X. W.; Li, Y. F. *Polym. Chem.* **2011**, *2*, 1678−1687. (g) Gu, Z. J.; Shen, P.; Tsang, S.-W.; Tao, Y.; Zhao, B.; Tang, P.; Nie, Y. J.; Fang, Y.; Tan, S. T. *Chem. Commun.* **2011**, *47*, 9381−9383.

(6) (a) Bijleveld, J.; Gevaerts, V. S.; Nuzzo, D. D.; Turbiez, M.; Mathijssen, S. G. J.; Leeuw, D. M.; Wienk, M. M.; Janssen, R. A. J. *Adv. Mater.* **2010**, *22*, E242−E246. (b) Jung, J. W.; Liu, F.; Russell, T. P.; Jo, W. H. *Energy Environ. Sci.* **2012**, *5*, 6857−6881. (c) Li, J.; Ong, K.-H.; Lim, S.-L.; Ng, G.-M.; Tan, H.-S.; Chen, Z.-K. *Chem. Commun.* **2011**, *47*, 9480−9482. (d) Bronstein, H.; Chen, Z. Y.; Ashraf, R. S.; Zhang, W. M.; Du, J. P.; Durrant, J. R.; Tuladhar, P. S.; Song, K.; Watkins, S. E.; Geerts, Y.; Wienk, M. M.; Janssen, R. A. J.; Anthopoulos, T.; Sirringhaus, H.; Heeney, M.; McCulloch, I. *J. Am. Chem. Soc.* **2011**, *133*, 3272−3275. (e) Qu, S. Y.; Tian, H. *Chem. Commun.* **2012**, *48*, 3039−3051. (f) Yiu, A. T.; Beaujuge, P. M.; Lee, O. P.; Woo, C. H.; Toney, M. F.; Frechet, J. M. *J. Am. Chem. Soc.* **2012**, *134*, 2180−2185.

(7) Huo, L. J.; Hou, J. H.; Chen, H.-Y.; Zhang, S. Q.; Jiang, Y.; Chen, T. L.; Yang, Y. *Macromolecules* **2009**, *42*, 6564−6571.

(8) Scharber, M. C.; Mühlbacher, D.; Koppe, M.; Denk, P.; Waldauf, C.; Heeger, A. J.; Brabec, C.-J. *Adv. Mater.* **2006**, *18*, 789−794.

(9) Jung, J. W.; Jo, J. W.; Liu, F.; Russell, T. P.; Jo, W. H. *Chem. Commun.* **2012**, *48*, 6933−6935.

(10) (a) Peet, J. M.; Senatore, L.; Heeger, A. J.; Bazan, G. C. *Adv. Mater.* **2009**, *21*, 1521−1527. (b) Moulé, A. J.; Meerholz, K. *Adv. Funct. Mater.* **2009**, *19*, 3028−3036.

(11) Cao, J. M.; Zhang, W.; Xiao, Z.; Liao, L. Y.; Zhu, W. G.; Zuo, Q. Q.; Ding, L. M. *Macromolecules* **2012**, *45*, 1710−1714.

(12) Zhang, Y.; Kim, C. K.; Lin, J.; Nguyen, T.-Q. *Adv. Funct. Mater.* **2011**, *22*, 97−105.